Free Electron Transfer with Bifunctional Donors: *p*-Aminotritylsilanes

Nikolaos Karakostas,[†] Sergej Naumov,[‡] and Ortwin Brede*[,†]

University of Leipzig, Wilhelm Ostwald Institute of Physical and Theoretical Chemistry, Linne'strasse 2, 04103 Leipzig, Germany, and Leibniz Institute of Surface Modification, Permoserstrasse 15, 04318 Leipzig, Germany

Received: July 31, 2009; Revised Manuscript Received: September 21, 2009

This work provides an in-depth look at the bimolecular free-electron transfer (FET) from bisubstituted (amine and -CR_2SiMe_3 groups) aromatic molecules to the solvent radical cations of *n*-BuCl. Because of the low rotational barriers, the substrates obtain all possible arrangements in solution. The electron jump is an unhindered process that does not require a defined encounter complex. The resulting radical cations show great conformer diversity because they directly inherit the geometry of their mobile precursors. One part of the radical cations is unstable and dissociates instantly, but the other one is metastable (microsecond lifetime). The two substituents reduce the barrier of internal rotation, resulting in stabilization of the otherwise good leaving group $-SiMe_3$. The amine group governs the reactivity of the system because it receives most of the electron density of the fluctuating highest MOs: primary and secondary amine groups lead to both instant and delayed formation of aminyl radicals; tertiary amines cause the rapid loss of an α-H^+ to yield α-aminoalkyl radicals.

1. Introduction

The liquid-state radical cations of alkanes and alkyl halides are metastable species with lifetimes of a few hundred nanoseconds. They can be generated conveniently by pulse radiolysis of their corresponding solutions (here *n*-BuCl, see eq 1). These parent radical cations are strong oxidizing agents[1] ionizing with diffusion-controlled reactions almost all solutes with an ionization potential lower than the solvents', as shown in eq 2. The particular phenomena associated with electron transfer in nonpolar media led to the introduction of the term free electron transfer (FET).

$$n\text{-BuCl} \rightsquigarrow [n\text{-BuCl}^{\bullet+} + e_{solv}] \rightarrow n\text{-BuCl}^{\bullet+}, Bu^{\bullet}, Cl^{-} \quad (1)$$

$$n\text{-BuCl}^{\bullet+} + D \rightarrow (FET) \rightarrow n\text{-BuCl} + D^{\bullet+} \text{ (D, electron donor)} \quad (2)$$

The electron transfer to solvent parent radical cations is a nonhindered process (i.e., the electron jumps from the solute molecule to the solvent cation regardless of the encounter geometry during their approach). Considering femtosecond oscillations, the dynamic mixture of conformers of D is subjected to vertical ionization. Therefore, the intramolecular dynamic motions define the conformation of the reactants as well as that of the immediate products.[2] The distribution of electron density in the highest molecular orbitals of monosubstituted aromatic substrates (similar to structure a in Scheme 1) varies considerably with the angle between the substituent and the aromatic ring.

In anilines, FET results in the direct synchronous formation of amine radical cations and aminyl radicals, as shown for diphenylamine in eq 3.[3,4]

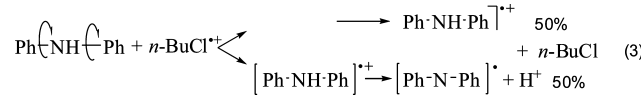

(3)

Depending on the angle of twist, the product radical cations can be metastable (distributed spin) or dissociative (localized spin density). The latter ones fragment before acquiring a favorable conformation during the internal nuclear reorganization that follows oxidation. Electron transfer involving various phenols[5,6] and other chalkogenols[7] gave similar results.

FET-generated radical cations of substituted benzylsilanes also exhibit a stability that is determined by the relative position (vertical or planar) between the $SiMe_3$ leaving group and the aromatic system.[8,9] Two reaction channels are observed here as well (eqs 4 and 5). For simplification, the manifold of dynamic conformers (in the momentum of the electron jump) can be classified by two extremes (i.e., vertical and planar types of donors):

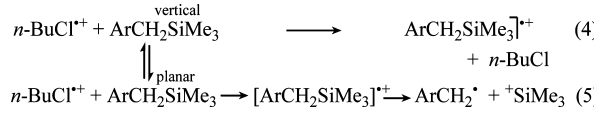

The diversity of molecules that have been subjected to FET with notable consequences raises an interesting question: What would be the influence of two different substituents that coexist on the same molecule? A suitable bifunctional system would

SCHEME 1

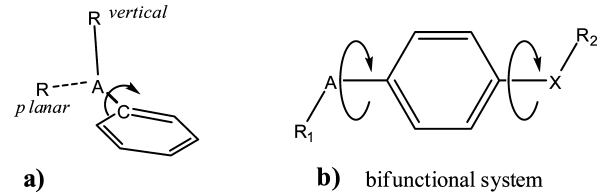

a) **b)** bifunctional system

* Corresponding author. E-mail: brede@uni-leipzig.de.
[†] University of Leipzig.
[‡] Leibniz Institute of Surface Modification

10.1021/jp9073569
Published on Web 10/22/2009

SCHEME 2

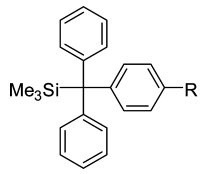

R: NEt_2, (1) NH_2, (2) NEtH, (3) NMe_2 (4)

contain two isolated mobile groups as depicted in Scheme 1b. In this article, we describe the particular aspects of FET in such electron-donor molecules.

The compounds of Scheme 2 bear silane and amine substituents. Their monosubstituted analogues have already been investigated.[3,8,9] Some of the properties of the molecules that have been associated with FET are the ionization potential of the ground state, the rotational barrier and dissociation energy of the weak bond, the spin density, and the frequencies of vibration of the radical cation. These properties vary within a desirable range between the two substituents that we chose to study.

2. Experimental Section

Pulse radiolysis experiments were performed with high-energy electron pulses (1 MeV, 15 ns duration) generated by pulse transformer accelerator ELIT (Institute of Nuclear Physics, Novosibirsk, Russia). Dosimetry was carried out using the absorption of the solvated electron in water as a calibration measurement. The dose delivered per pulse was usually around 100 Gy (generating $\sim 10^{-5}$ mol dm^{-3} primary n-BuCl$^{\bullet+}$). Detection of the transient species was carried out by an optical absorption setup consisting of a pulsed xenon lamp (XBO 450, Osram), a SpectraPro-500 monochromator (Acton Research Corporation), an R955 photomultiplier (Hamamatsu Photonics), and a 1 GHz digitizing oscilloscope (TDS 640, Tektronix). Further details are given elsewhere.[10] The solutions were continuously passed through the sample cell. The optical path length was 1 cm.

n-Butyl chloride was purified by treatment with molecular sieves (A4, X13) and distillation under nitrogen as described previously.[10,11] The *p*-(Diphenylmethyl)anilines used (Scheme 2) where synthesized according to the literature.[12]

Photolysis experiments employed the fourth harmonic (266 nm) of a Quanta-Ray GCR-11 Nd:YAG laser (Spectra Physics). Pulses of <3 ns duration (fwhm) with energies of 1 mJ were used. The optical detection system was similar to that described above for the radiolysis apparatus.

Quantum chemical calculations were performed with density functional theory (DFT) hybrid B3LYP[13−15] methods and the standard 6-31G(d) basis set as implemented in the Gaussian 03 program.[16]

3. Results

Experimental Approach. The radiolysis of *n*-BuCl yields solvent radical cations (cf. reaction 1). The optical absorption spectrum of *n*-BuCl$^{\bullet+}$ consists of a broad band with λ_{max} around 500 nm and a lifetime of about 100 ns. A quencher present in millimolar concentration would limit this lifetime (according to eq 2 to a few nanoseconds[17]) as a result of rapid free electron transfer.

Laser photolysis provides an alternative way to produce transients and to record their spectral and kinetic properties selectively. Hence, it is employed as a technique (complementary to pulse radiolysis) for the identification of transients masked by overlapping absorptions.

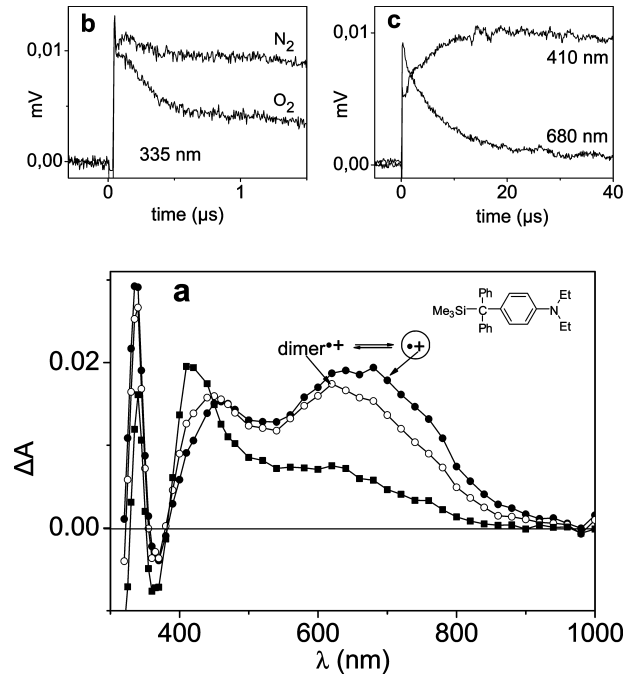

Figure 1. Absorption spectra recorded after pulse radiolysis of a 1×10^{-3} mol dm^{-3} solution of 4-(diphenyl(trimethylsilyl)methyl)-*N*,*N*-diethylaniline (**1**) in *n*-BuCl saturated with N_2: (•) 800 ns, (○) 2 μs, and (■) 10 μs after the pulse (a). Time profiles derived at 335 nm under N_2 and O_2 atmospheres (b) and at 410 and 680 nm under N_2 (c).

Pulse Radiolysis Experiments. ***4-(Diphenyl(trimethylsilyl) methyl)-N,N-diethylaniline (1).*** After a nitrogen-purged solution of 10^{-3} mol dm^{-3} **1** was pulsed, the solvent radical cation (λ_{max} = 500 nm) decays with the simultaneous formation of radical cation **1**$^{\bullet+}$ and radicals derived from **1**. The broad band at 680 nm (Figure 1a), the one at 450 nm, and part of the sharp peak at 335 nm have been assigned to **1**$^{\bullet+}$. Furthermore, partially from the very beginning, a radical absorption placed in the 330−450 nm range is observed. Depletion around 365 nm as a result of the consumption of the parent molecule complicates the analysis of this spectral area.

Radical Cations. For time up to 2 μs, a spectral shift of the maximum from 680 to 620 nm can be observed. The rate of the underlying process is dependent upon the parent molecule concentration. As in the case of various charge-transfer complexes known from the literature,[18,19] it is attributed to the progressive achievement of equilibrium between the monomeric and the dimeric form of the radical cation:

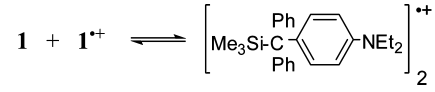

(6)

Radicals. As already mentioned, a part of the radical absorption appears from the very beginning and leads to less-specific background absorption. However, the decay of the cationic species (lifetime 7 μs) is connected to the formation of a transient with λ_{max} at 410 and 340 nm (isosbestic point at 450 nm). This is illustrated by the time profiles given in Figure 1c.

The delayed process is associated with the desilylation of **1**$^{\bullet+}$ and the production of the 4-*N*,*N*-diethylaminotrityl radical (eq 7). Oxygen eliminates the above-mentioned transient but has a marginal effect on the radical cation. A further verification of the identity of the species comes from the Stern−Volmer

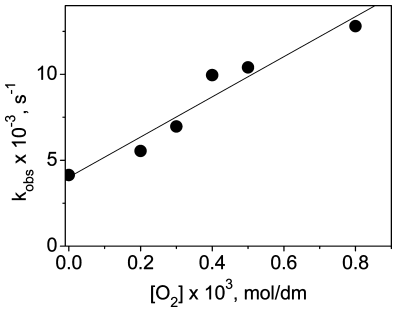

Figure 2. Plot of the pseudo-first-order rate constant for decay at 410 nm after pulse radiolysis of a 1×10^{-3} mol dm^{-3} solution of **1** in *n*-BuCl as a function of O_2 concentration.

plot in Figure 2. The rate constant ($k_8 = 1.2 \times 10^7$ dm^3 mol^{-1} s^{-1}) for the reaction with oxygen at 410 nm is characteristic of trityl-type radicals.[20,21] The weak absorption of these trityl radicals is explained by the competing neutralization: $\mathbf{1}^{\bullet+} + Cl^- \rightarrow$ products. (See also the Discussion.)

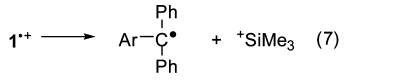

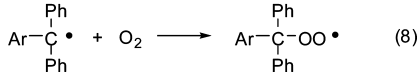

With regard to the radical background observed at the UV border of the spectrum, a second effect of oxygen can be seen at 335 nm. It corresponds to a much faster process ($k_9 \geq 6 \times 10^8$ dm^3 mol^{-1} s^{-1}) that is presented in Figure 1b and is attributed to the reaction of oxygen with the rapidly formed α-aminoalkyl radical, which is the deprotonation product of dissociative cation $\mathbf{1}^{\bullet+}$. Rates of the same magnitude were reported, for example, for the reaction of oxygen with the radiolytically generated α-aminoalkyl radicals of dimethylamine (2×10^9 dm^3 mol^{-1} s^{-1})[3] and 1,2,2,6,6-pentamethylpiperidine (3×10^8 dm^3 mol^{-1} s^{-1}).[22]

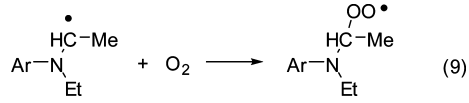

4-(Diphenyl(trimethylsilyl)methyl)aniline (2). Pulse radiolysis of **2** in *n*-BuCl results in the formation of the corresponding FET products. The spectra of a 1 mM solution of **2** in a nitrogen atmosphere are shown in Figure 3a. Under these conditions, the lifetime of parent *n*-$BuCl^{\bullet+}$ is limited (cf. eq 2) to ~50 ns ($k \approx 1.7 \times 10^{10}$ dm^3 mol^{-1} s^{-1}) and can be observed as a spike in Figure 3b at 600 nm.

The absorption of radical cation $\mathbf{2}^{\bullet+}$ consists of a narrow intense band at 320−325 nm and a broad one extending from 650 to 1000 nm. It overlaps with a second transient, especially at the short-wavelength peak; therefore, the 0.8 μs lifetime of $\mathbf{2}^{\bullet+}$ is derived at 800 nm in Figure 3b. The decay of $\mathbf{2}^{\bullet+}$ is not sensitive to oxygen. It can be associated with the presence of nucleophiles such as Cl^-. A significant number of chloride anions are certainly produced after the radiolysis of *n*-BuCl (eq 1), and further addition of the anion in the form of Bu_4NCl accelerates deprotonation reaction 10.

$$ArNH_2^{+\bullet} + Cl^- \rightarrow ArNH^{\bullet} + HCl,\ k = 2 \times 10^9\ dm^3\ mol^{-1}\ s^{-1} \quad (10)$$

The aminyl radical of **2** is the second transient formed via the described electron transfer. Under an N_2 atmosphere, it decays slowly with second-order kinetics. Its spectrum is the residue absorption of Figure 3a (10 μs line) with maxima at 335 and 640 nm. As a nitrogen-centered radical, it is less reactive toward oxygen (eq 11) than is a carbon-centered one (e.g., eq 8):

$$ArHN^{\bullet} + O_2 \rightarrow ArHNOO^{\bullet},\ k = 2 \times 10^6\ dm^3\ mol^{-1}\ s^{-1} \quad (11)$$

There is kinetic evidence of the formation of the aminyl radical through two separate channels: a single-step route that includes FET and the immediate loss of a proton from **2** as well as the delayed nucleophile-assisted deprotonation of metastable radical cation $\mathbf{2}^{\bullet+}$. There is an analogy with the previously described pattern in reaction 3. This behavior will be elucidated in the Discussion section.

4-(Diphenyl(trimethylsilyl)methyl)-N-ethylaniline (3). When a 1 mM solution of **3** in nitrogen-purged *n*-BuCl is subjected to pulse radiolysis, then FET to parent *n*-$BuCl^{\bullet+}$ results in the formation of three distinct bands with λ_{max} at 330, 450, and 680 nm (cf. Figure 4).

The early-time spectrum consists of the combined absorptions of two transients assigned to the radical cation of parent molecule $\mathbf{3}^{\bullet+}$ and the aminyl radical of **3** produced by immediate deprotonation of the dissociative radical cation. Metastable radical cation $\mathbf{3}^{\bullet+}$ is converted ($\tau = 3$ μs) to the long-lasting N-centered radical by the loss of a proton in a reaction similar to eq 10. Therefore, the residual spectral peaks (taken 4 μs after the pulse) at 330, 620, and 460 nm belong to the aminyl radical

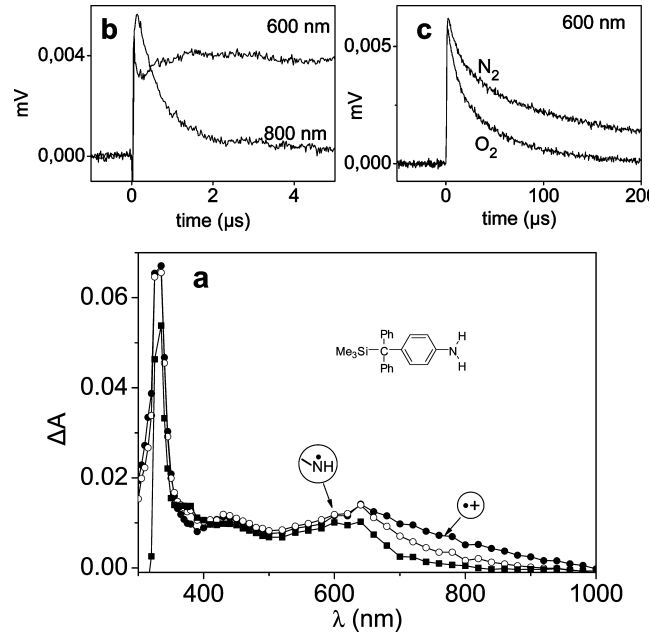

Figure 3. Time-resolved absorption spectra observed after pulse radiolysis of a 1×10^{-3} mol dm^{-3} solution of 4-(diphenyl(trimethylsilyl)methyl)aniline (**2**) in N_2-purged *n*-BuCl: (•) 0.8 μs, (○) 1.5 μs, and (■) 10 μs after the pulse (a). Formation of the aminyl radical at 600 nm and the decay of the $\mathbf{2}^{\bullet+}$ radical cation at 800 nm (b). Time profiles taken at 600 nm under N_2 and O_2 atmospheres (c).

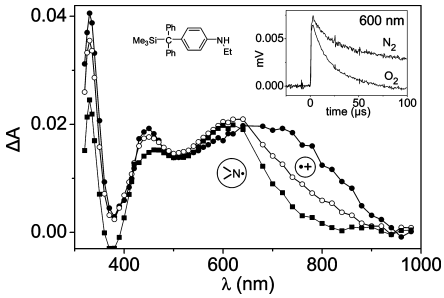

Figure 4. Transient absorption spectra obtained on pulse radiolysis of a 1×10^{-3} mol dm^{-3} solution of 4-(diphenyl(trimethylsilyl)methyl)-*N*-ethylaniline (**3**) in *n*-BuCl saturated with N_2: (•) 300 ns, (○) 1 μs, and (■) 4 μs after the pulse. (Inset) Time profiles at 600 nm (N_2 and O_2 atmospheres).

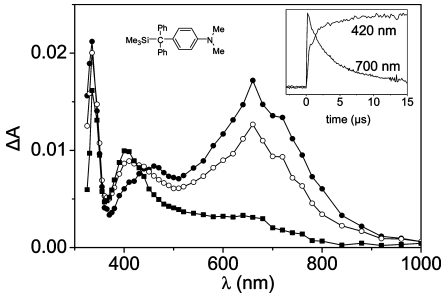

Figure 5. Absorption spectra recorded after pulse radiolysis of a 1×10^{-3} mol dm^{-3} solution of 4-(diphenyl(trimethylsilyl)methyl)-*N*,*N*-dimethylbenzenamine (**4**) in *n*-BuCl saturated with N_2: (•) 800 ns, (○) 2 μs, and (■) 10 μs after the pulse. (Inset) Time profiles at 420 and 700 nm (with normalized amplitude).

that is formed from both paths. This argumentation is further supported by the slow quenching effect of oxygen seen in the inset of Figure 4.

4-(Diphenyl(trimethylsilyl)methyl)-N,N-dimethylbenzenamine (4). Pulse radiolysis of a 1×10^{-3} mol dm^{-3} solution of **4** in N_2-purged *n*-BuCl results in the spectra given in Figure 5. Initially, two absorption bands (with λ_{max} at 335 nm and 660 nm) were formed, which we assign to radical cation **4**$^{\bullet+}$. The decay of **4**$^{\bullet+}$ takes place with the same time law ($\tau = 4.5$ μs) as the formation of a new band at 410 nm (inset of Figure 5). It originates from the dissociation of the C−Si bond (as in eq 7) and corresponds to the dimethylaminotrityl radical.[23]

The behavior of **4** after FET is similar to that of **1**, but it is not identical. FET results in the generation of metastable radical cations as well as C-centered radicals. Consequently, (much) delayed desilylation happens with the formation of trityl-type

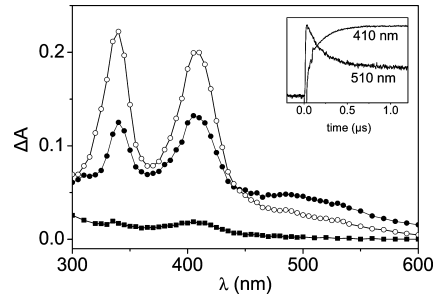

Figure 6. Transient spectra following 266 nm laser irradiation of a 1×10^{-4} mol dm^{-3} solution of 4-(diphenyl(trimethylsilyl)methyl)-*N*,*N*-diethylbenzenamine (**1**) in acetonitrile recorded (•) 300 ns, (○) 1 μs (under an N_2 atmosphere), (■) 1 μs (under O_2) after the pulse. (Inset) Time profiles under N_2 at 405 and 510 nm with normalized amplitude.

SCHEME 3

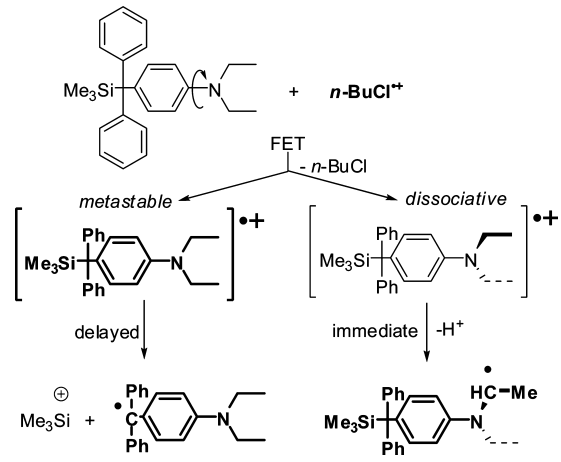

radicals. Comparison with **1** shows that the production of α-aminoalkyl radicals is less favored in the case of **4**. Furthermore, the dimerization of the radical cation was not identified in the spectra.

Laser Photolysis. ***4-(Diphenyl(trimethylsilyl)methyl)-N,N-diethylaniline (1).*** Laser photolysis at 266 nm of a nitrogen-saturated solution of **1** (1×10^{-4} mol dm^{-3}) in acetonitrile yields the spectra given in Figure 6. The time window of 300 ns after the shot consists of twin peaks with maxima at 330 and 410 nm and a weaker broad band in the range between 450 and 550 nm. The latter one decays with first-order kinetics ($k = 4.7 \times 10^6$ s^{-1}), which match the increase of the absorption of the two shorter-wavelength bands. This can be seen in the inset of Figure 6 (fluorescence distorts the first 100 ns at 410 nm). The broad band belongs to the triplet state (T_1) of the parent molecule. It is involved in the photodissociation of the C−Si bond and the production of the *p*-(diethylamino)-triphenylmethyl radical according to reaction 12.

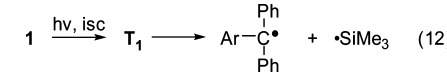

Oxygen, which is a quencher for triplet states and radicals, provided an additional means of identification for the transients. The peaks at 330 and 410 nm are attributed to the *p*-(diethylamino)-triphenylmethyl radical in agreement with the assignment made after the pulse radiolysis study of **1**.

4. Discussion

Previous studies of the free electron transfer from benzyltrimethylsilanes (Ar−CR_2SiMe_3) to solvent ions (*n*-BuCl$^{\bullet+}$) have

SCHEME 4

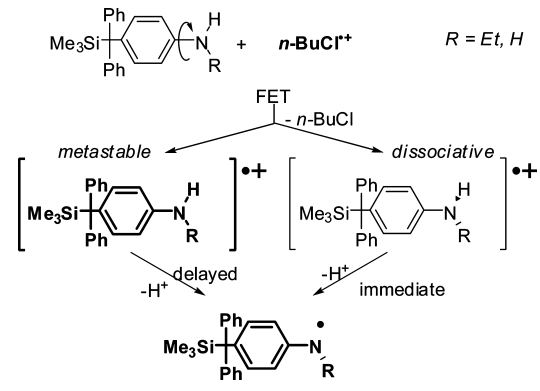

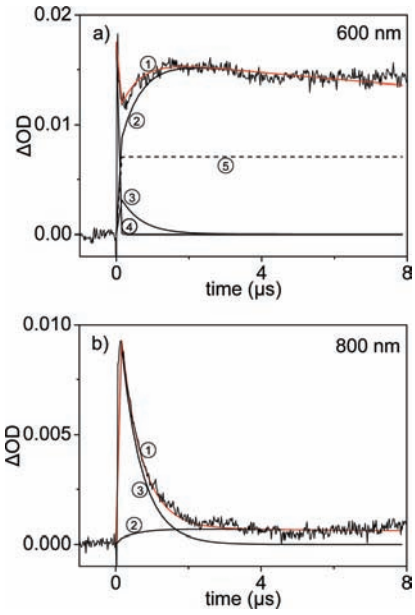

Figure 7. Experimental time profiles for a 1×10^{-3} mol dm^{-3} solution of **2** in *n*-BuCl under N_2 and simulated curves at 600 (a) and 800 nm (b): (1) experimental curves, (2) aminyl radical, (3) radical cation $\mathbf{2}^{\bullet+}$, (4) *n*-BuCl$^{\bullet+}$, and (5) rapidly formed portion of an aminyl radical.

revealed the existence of two separate reaction paths that lead to the formation of radicals (eqs 4 and 5).[8,24] They were attributed to the initial generation of radical cations that exhibit either dissociative or metastable behavior depending on their conformation. The substantial mobility of the CR_2SiMe_3 group allows the existence of different rotamers of the parent molecule in solution. Additionally, the electron-transfer step is faster than the relaxation process of the substrates and does not favor any particular orientation.[9] The dissociation of the unstable radical cations is instantaneous whereas that of the metastable transients takes place much more slowly.

The introduction of an amino group in the para position alters the reaction scheme. Apparently, there is no instantaneous C−Si bond fragmentation among the compounds in this study. The experiment has shown that the diethylaminotrityl radical is produced only from metastable cations by a delayed process that falls into the time range of microseconds (Figure 1). However, the unstable dissociative radical cations decay by rapid deprotonation. This particular behavior of silylated anilines is in contrast to the findings for the bisubstituted 4-hydroxythiophenol where both −OH and −SH groups participate in rapid FET reactions.[25] In a competition between the two mobile groups of an unstable radical cation, the dissociation preferably takes place at the group that provides the deepest potential trap. In 4-thiophenol, the groups appear to be almost equivalent (e.g., $IP_{phenol} - IP_{thiophenol} \approx 0.2$ eV)[26,27] whereas in silylated amines the aniline group is low enough to quench the $SiMe_3$ (e.g., $IP_{benzyltrimethylsilane} - IP_{aniline} \approx 0.6$).[28,29]

Tertiary amines **1** and **4** yield α-aminoalkyl radicals (case (i), Scheme 3) whereas primary and secondary amines **2** and **3** form aminyl radicals (case (ii), Scheme 4). The experimental results point toward the existence of multiple (different) reaction channels originating from the elementary step of the electron jump.

Case (i): The reaction sequence of Scheme 3 illustrates the scenario for the tertiary amines applied to **1**. Dimethylamino homologue **4** exhibits similar behavior, with a less-efficient deprotonation route. Scheme 3 could contain the neutralization of the metastable cations by Cl^-, which competes with the delayed desilylation. That reaction partially explains the relatively weak signals of the trityl radicals in the radiolysis experiments (Figure 1) in comparison with photolysis (Figure 6). A second cause is simply the fact that the initial concentration of *n*-BuCl$^{\bullet+}$ in our system is $\sim 1 \times 10^{-5}$ mol dm^{-3} (i.e., an order on magnitude lower than the concentration of **1** used for photolysis).

Case (ii): The FET ionization of **2** and **3** triggers the loss of a proton attached to the N atom. The aminyl radical is produced both directly (during electron transfer) as well as by a slower reaction that is observable on the microsecond timescale. Eventually, the overall process does not involve the dissociation of the weak C−Si bond, as can be seen in Scheme 4. Under similar conditions, the radical cation of unsubstituted tritylmethylsilane ($Ph_3C-SiMe_3$) has a lifetime shorter than 70 ns.[8]

FET versus Reaction-Controlled Electron Transfer. The ground-state molecules with unhindered torsion and bending motions ($E_a \leq 20$ kJ/mol) experience practically free mobility. In contrast, their cations are more rigid with much higher rotational barriers.

FET in nonpolar systems exhibits some peculiarities.[5,17] A number of basic aspects can be summarized as follows: (a) the reactants are only weakly solvated and hence interaction with the solvent during the transfer is negligible; (b) the electron jump itself is an instantaneous process; and (c) in conjunction with the previous two points, free-electron transfer occurs without any preassociation between the reactants (i.e., with no defined encounter complex).

When two reactants form an encounter complex by approaching each other, then a rigid structure including the mesomeric arrangement is shaped under energetic optimization. After this state is prepared, the e-jump can happen under favorable conditions. In our previous studies, we have been able to distinguish these two possibilities: FET as a one-collision event and reaction-controlled electron transfer, depending on the free energy of the electron transfer.[6,30] For that purpose, we utilized an electron acceptor with an electron affinity lower than that of BuCl$^{\bullet+}$, which at the same time had the capability to generate $\pi\pi$ complexes with the electron donor.

The electron donors in FET undergo vertical ionization; therefore, the radical cation that is produced maintains the conformation of the ground-state molecule. The substrates

TABLE 1: Spectral and Kinetic Data of Product Formation by Free-Electron Transfer

		cationic species		radicals	
compound	k of FET (dm^3 mol^{-1} s^{-1})	λ_{max} (nm)	τ_{decay} (μs)	λ_{max} (nm)	k_{O_2} (dm^3 mol^{-1} s^{-1})
1	2.3×10^{10}	335, 450, 680	7.0	340, 410	1.2×10^{7a}
2	1.7×10^{10}	320, 430, 700	0.8	335, 640	2×10^{6b}
3	2.1×10^{10}	330, 450, 680	3.0	330, 620	3×10^{6b}
4	1.9×10^{10}	335, 450, 660	4.5	335, 410	1.1×10^{7a}
Ph_3C-$SiMe_3$	5×10^{9c}	480−520^c	<0.07^c	340^c	7×10^{8c}

[a] Reaction with a C-centered radical. [b] Reaction with an N-centered radical. [c] From ref 8.

studied in this article have two bonds exhibiting a twisting, or torsional, motion relative to the rest of the molecule (i.e., the $C_{Ar}-C_{sp^3}$ (benzylic) and the $C_{Ar}-N$ bond. In liquid-state solutions, all possible spatial arrangements with respect to the aromatic ring coexist.

Interpretation of FET Kinetics. Spectral superposition of the transients hinders the study of the radical cation and the aminyl radical of the molecule at separate wavelengths. The involvement of a rapid and a delayed reaction in the formation of the aminyl radical (of **2** and **3**) would contribute to the reaction-time evolution with an initial steep part followed by a well-resolved built-up part. However, there is no convenient wavelength for the direct observation of that behavior. Therefore, the time profiles of the overlapping transients were simulated using numerical integration with a modified version of ACUCHEM.[31] The reaction scheme is described by eqs 13−20 given below (where $R-NH_2$ is **2**):

$$n\text{-BuCl} \rightsquigarrow n\text{-BuCl}^{\bullet+} + e_{solv}^{-} \quad (13)$$

$$n\text{-BuCl} + e_{solv}^{-} \rightarrow n\text{-Bu}^{\bullet} + Cl^{-} \quad (14)$$

$$n\text{-BuCl}^{\bullet+} \rightarrow \text{products} \quad (15)$$

$$n\text{-BuCl}^{\bullet+} + \text{R-NH}_2 \rightarrow [\text{R-NH}_2]^{\bullet+}_{(\text{unstable})} + n\text{-BuCl} \quad (16)$$

$$n\text{-BuCl}^{\bullet+} + \text{R-NH}_2 \rightarrow [\text{R-NH}_2]^{\bullet+}_{(\text{metastable})} + n\text{-BuCl} \quad (17)$$

$$[\text{R-NH}_2]^{\bullet+}_{(\text{unstable})} \rightarrow \text{R-NH}^{\bullet} + H^{+} \quad (18)$$

$$[\text{R-NH}_2]^{\bullet+}_{(\text{metastable})} + Cl^{-} \rightarrow \text{R-NH}^{\bullet} + H^{+}\cdots Cl^{-} \quad (19)$$

$$\text{R-NH}^{\bullet} + \text{R-NH}^{\bullet} \rightarrow \text{dimer} \quad (20)$$

Using multiple wavelengths for simulation improves the accuracy of the procedure. Figure 7 shows the resulting curves at 600 and 800 nm drawn together with the corresponding experimental profiles. $BuCl^{\bullet+}$ is present only as a spike during the first nanoseconds after the pulse in Figure 7a. The aminyl radical is the strongest absorbing transient at 600 nm. The rapidly produced portion is depicted by the dashed line (5) in Figure 7a. It represents ∼40% of the total amount of the radical derived from **2**. In the case of **3**, the simulation of the experimental time profiles is achieved with an ∼30% contribution of the rapid part of eq 18.

The substrates that contain a tertiary amine group (**1** and **4**) yield the α-aminoalkyl radicals with the same time law as the FET (Figure 1b). It appears that ionization and generation of the radical (from the dissociative radical cations) proceed in a single step. However, the metastable radical cations are slowly neutralized while desilylation is also observed as a secondary reaction. A reliable calculation of the proportion between dissociative and metastable radical cations would require the extinction coefficients of their products. On the basis of the typical extinction coefficient values for trityl radicals (∼36 000 mol^{-1} dm^3 cm^{-1})[32] and up to a 1×10^{-5} mol dm^{-3} concentration

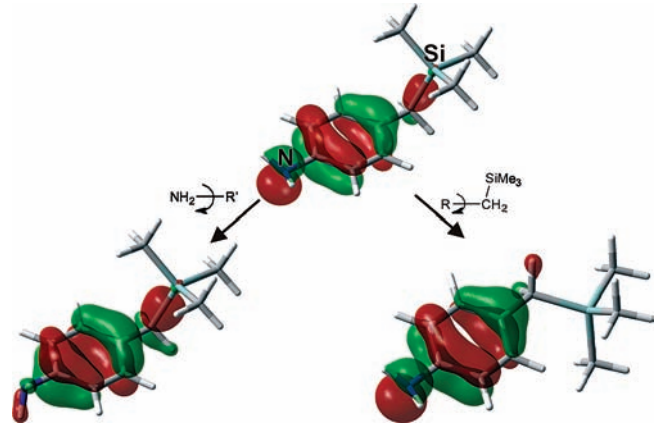

Figure 8. Transformation of HOMO of the 4-((trimethylsilyl)-methyl)aniline (**5**) singlet ground state (isodensity 0.05) upon the formation of (H_2N- and $-CH_2SiMe_3$) transition states.

of $n\text{-BuCl}^{\bullet+}$ in our system, we can estimate a 10% desilylation for **1** and 5% for **4**. That is approximately the analogy between the lifetimes of the metastable radical cations presented in Table 1. As we move from primary amine **2** to secondary **3** and finally to tertiary **4** and **1**, there is a tendency for longer lifetimes of the metastable radical cations.

Analysis of FET with Quantum Chemical Calculations. A better understanding of the experimental observations can be achieved by quantum calculations. The behavior of the amino part of the molecules under FET is in good agreement with the findings of previous works on anilines.[3,4,33] The contribution of the $SiMe_3$ group to free-electron transfer was not equally clear. Analogous silylated substrates under similar experimental conditions have demonstrated a rapid dissociation of the C−Si bond with up to 75% yield.[8] We selected some model molecules, which could explain the effect in FET of two substituents connected to a single ring. Subsequently, we used the DFT B3LYP/6-31G(d) method to obtain information regarding the radical cations as well as the neutral molecules. The simplest prototype for silylated anilines (i.e., 4-((trimethylsilyl)-methyl)aniline (**5**)) is compared with that for aniline and benzyltrimethylsilane ($PhCH_2SiMe_3$).

Figure 8 shows the fluctuation of electron density on structures that correspond to the most characteristic rotamers. The highest doubly occupied MOs (HOMO) of the singlet ground state are certainly involved in the electron-transfer process. As can be noted from Table 2, the vibrational oscillations are at least 10 times faster than the rotation of the mobile group (but both of them are postulated to be slower than the electron-transfer jump). That is roughly the time window for the unstable radical cations to dissociate. FET fragmentation (by vibrational motion[2] in the femtosecond range) should be faster than the accomplishment of the tortional oscillations. Scheme 5 demonstrates the energy barriers the molecules have to overcome for internal rotation.

The properties of neutral molecules do not show a significant differentiation for the following reasons: (a) Aniline has barrier comparable (21.3 kJ mol^{-1}) to that of the $-NH_2$ substituent of **5** (18.4 kJ mol^{-1}). Additionally, benzyltrimethylsilane (14.6 kJ mol^{-1}) is very close to the barrier of the $-CH_2SiMe_3$ substituent of **5** (13.0 kJ mol^{-1}). (b) The BDE of the benzyltrimethylsilane C−Si bond (300.6 kJ mol^{-1}) is similar to that of **5** (293.1 kJ mol^{-1}).

However, the barrier of radical cation $\mathbf{5}^{\bullet+}$ receives significant stabilization over those of aniline and benzyltrimethylsilane. Hence, the $-NH_2$ substituent of **5** requires 102.1 kJ mol^{-1} to

TABLE 2: Calculated Parameters of Substituted Benzenes in Their Singlet and Radical Cation States[a]

	singlet			radical cation		
compound	$E_{a(ZP)}$ (kJ mol^{-1})	τ_{rot} (fs)	τ_{vibr} (fs)	$E_{a(ZP)}$ kJ mol^{-1})	spin on C_{Ar}−Si	spin on C_{Ar}−N
aniline	21.3	119	9	146.4		0.443793
benzyltrimethylsilane	14.6	547	37(C−Si)	65.7	0.31061	
silylaniline (at Ar−CH_2SiMe_3)	13.0	1112 (Ar−C)	37(C−Si)	36.4	0.126882	
silylaniline (at Ar′−NH_2)	18.4	128 (Ar′−N)	9(N−H)	102.1		0.405591
4 (at Ar−CPh_2SiMe_3)	13.8	2085 (Ar−C)	4(C−Si)	23.0	0.152426	
4 (at Ar′−NMe_2)	<8.4[b]	629 (Ar′−N)		129.7		0.322518

[a] $E_{a(ZP)}$ (kJ mol^{-1}), the activation energy (zero-point-energy-corrected) of rotational motion along the Ar−X (X = N, C) axis; time of rotation; vibrational motion; and spin density. [b] The structure with $N(Me)_2$ perpendicular to Ar is stable (not the transition state) in this case.

SCHEME 5: DFT B3LYP 6-31G(d)-Calculated Rotational Barriers of Mono- and Bisubstituted Benzenes

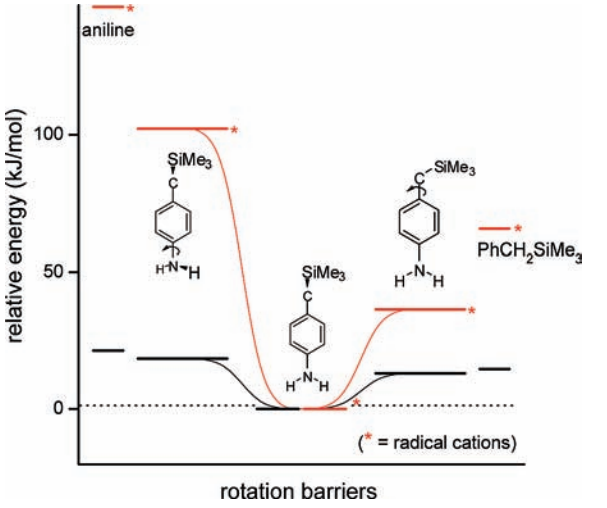

obtain the transition state, which is much lower than the value calculated for aniline (146.4 kJ mol^{-1}). The same trend is seen on the $-CH_2SiMe_3$ side of **5** with a 36.4 kJ mol^{-1} rotational barrier that is considerably smaller than that of benzyltrimethylsilane (65.7 kJ mol^{-1}).

The spin density of the radical cation is shifted to the amine side of the molecules, making the $SiMe_3$ part less sensitive to the ionization process. The activation barrier can be the driving force for the subsequent rapid fragmentation of a radical cation (if generated in an unfavorable geometry). Furthermore, in the bifunctional molecules, such as those studied in this article, there is a competition between the silane and the aniline part of the radical cation. Even though the $SiMe_3$ substituent does not exhibit rapid dissociation, the amine part maintains the instant deprotonation behavior (Schemes 3 and 4) of FET. The substituent with the deepest potential trap (N atom) more efficiently binds the spin density of the highest MOs. As a result, the rotation about the C_{Ar}−N bond leads to greater changes in the electron distribution and localizes the additional destabilization of the radical cation in the vicinity of the amine group.

5. Conclusions

We explored the free-electron transfer to parent *n*-BuCl radical cations from molecules that combine two mobile substituents: one amine and one $-CR_2SiMe_3$ group that coexist on the same aromatic ring. Their rotational barrier allows the formation of an extended diversity of conformers. This diversity is directly projected to their radical cations because the ionization process in FET is vertical. Depending on the orientation of their substituents, the radical cations can be classified as metastable, with lifetimes of microseconds, or unstable, which dissociate during the internal dynamic motion (on the femtosecond timescale). The deepest potential trap (i.e., the amine group) determines the behavior of the radical cation. The instant dissociation of the weak C−Si bond (known from previous studies[8,9,24]) is eliminated, and the much slower desilylation process was observed only on molecules with tertiary amines. This result is associated with the relatively low rotational barriers of the radical cations. The amine group maintains its particular FET properties. Radical cations of primary and secondary amines undergo rapid, delayed deprotonation toward aminyl radicals, whereas tertiary amines instantly form α-aminoalkyl radicals by ejecting a proton.

References and Notes

(1) Dorfman, L. M. *Acc. Chem. Res.* **1970**, *3*, 224.
(2) Brede, O.; Naumov, S. *J. Phys. Chem. A* **2006**, *110*, 11906.
(3) Maroz, A.; Hermann, R.; Naumov, S.; Brede, O. *J. Phys. Chem. A* **2005**, *109*, 4690.
(4) Brede, O.; Maroz, A.; Hermann, R.; Naumov, S. *J. Phys. Chem. A* **2005**, *109*, 8081.
(5) Brede, O.; Hermann, R.; Naumann, W.; Naumov, S. *J. Phys. Chem. A* **2002**, *106*, 1398.
(6) Brede, O.; Naumov, S.; Hermann, R. *Radiat. Phys. Chem.* **2003**, *67*, 225.
(7) Brede, O.; Mahalaxmi, G. R.; Naumov, S.; Naumann, W.; Hermann, R. *J. Phys. Chem. A* **2001**, *105*, 3757.
(8) Brede, O.; Hermann, R.; Naumov, S.; Zarkadis, A. K.; Perdikomatis, G. P.; Siskos, M. G. *Phys. Chem. Chem. Phys.* **2004**, *6*, 2267.
(9) Karakostas, N.; Naumov, S.; Siskos, M. G.; Zarkadis, A. K.; Hermann, R.; Brede, O. *J. Phys. Chem. A* **2005**, *109*, 11679.
(10) Mahalaxmi, G. R.; Hermann, R.; Naumov, S.; Brede, O. *Phys. Chem. Chem. Phys.* **2000**, *2*, 4947.
(11) Mehnert, R.; Brede, O.; Naumann, W. *Ber. Bunsen-Ges. Phys. Chem.* **1982**, *86*, 525.
(12) Siskos, M. G.; Garas, S. K.; Zarkadis, A. K.; Bokaris, E. P. *Chem. Ber.* **1992**, *125*, 2477.
(13) Becke, A. D. *J. Chem. Phys.* **1993**, *98*, 5648.
(14) Becke, A. D. *J. Chem. Phys.* **1996**, *104*, 1040.
(15) Lee, C.; Yang, W.; Parr, R. G. *Phys. Rev. B* **1988**, *37*, 785.
(16) Frisch, M. J.; Trucks, G. W.; Schlegel, H. B.; Scuseria, G. E.; Robb, M. A.; Cheeseman, J. R.; Zakrzewski, V. G.; Montgomery, J. A., Jr; Stratmann, R. E.; Burant, J. C.; Dapprich, S.; Millam, J. M.; Daniels, A. D.; Kudin, K. N.; Strain, M. C.; Farkas, O.; Tomasi, J.; Barone, V.; Cossi, M.; Cammi, R.; Mennucci, B.; Pomelli, C.; Adamo, C.; Clifford, S.; Ochterski, J.; Petersson, G. A.; Ayala, P. Y.; Cui, Q.; Morokuma, K.; Salvador, P.; Dannenberg, J. J.; Malick, D. K.; Rabuck, A. D.; Raghavachari, K.; Foresman, J. B.; Cioslowski, J.; Ortiz, J. V.; Baboul, A. G.; Stefanov, B. B.; Liu, G.; Liashenko, A.; Piskorz, P.; Komaromi, I.; Gomperts, R.; Martin, R. L.; Fox, D. J.; Keith, T.; Al-Laham, M. A.; Peng, C. Y.; Nanayakkara, A.; Challacombe, M.; Gill, P. M. W.; Johnson, B.; Chen, W.; Wong, M. W.; Andres, J.; Gonzalez, C.; Head-Gordon, M.; Replogle, E. S.; Pople, J. A. *Gaussian 03*, revision B.02; Gaussian: Pittsburgh, PA, 2003.
(17) Brede, O. *Res. Chem. Intermed.* **2001**, *27*, 709.
(18) Rodgers, M. A. J. *J. Chem. Soc., Faraday Trans. 1* **1972**, *68*, 1278.
(19) Egusa, S.; Arai, S.; Kira, A.; Imamura, M.; Tabata, Y. *Radiat. Phys. Chem.* **1977**, *9*, 419.
(20) Maillard, B.; Ingold, K. U.; Scaiano, J. C. *J. Am. Chem. Soc.* **1983**, *105*, 5095.
(21) Siskos, M. G.; Zarkadis, A. K.; Steenken, S.; Karakostas, N.; Garas, S. K. *J. Org. Chem.* **1998**, *63*, 3251.
(22) Brede, O.; Beckert, D.; Windolph, C.; Göttinger, H. A. *J. Phys. Chem. A* **1998**, *102*, 1457.

(23) Tasis, D. A.; Siskos, M. G.; Zarkadis, A. K.; Steenken, S.; Pistolis, G. *J. Org. Chem.* **2000**, *65*, 4274.
(24) Brede, O.; Hermann, R.; Naumov, S.; Perdikomatis, G. P.; Zarkadis, A. K.; Siskos, M. G. *Chem. Phys. Lett.* **2003**, *376*, 370.
(25) Dey, G. R.; Hermann, R.; Naumov, S.; Brede, O. *Chem. Phys. Lett.* **1999**, *310*, 137.
(26) Fuke, K.; Yoshiuchi, H.; Kaya, K.; Achiba, Y.; Sato, K.; Kimura, K. *Chem. Phys. Lett.* **1984**, *108*, 179.
(27) Ashby, M. T.; Enemark, J. H.; Lichtenberger, D. L. *Inorg. Chem.* **1988**, *27*, 191.
(28) Distefano, G.; Pignataro, S.; Ricci, A.; Colonna, F. P.; Pietropaolo, D. *Ann. Chim.* **1974**, *64*, 153.
(29) Meek, J. T.; Sekreta, E.; Wilson, W.; Viswanathan, K. S.; Reilly, J. P. *J. Chem. Phys.* **1985**, *82*, 1741.
(30) Karakostas, N.; Naumov, S.; Brede, O. *J. Phys. Chem. A* **2007**, *111*, 71.
(31) Braun, W.; Herron, J. T.; Kahaner, D. K. *Int. J. Chem. Kinet.* **1988**, *20*, 51.
(32) Bartl, L.; Steenken, S.; Mayr, H.; McClelland, R. A. *J. Am. Chem. Soc.* **1990**, *112*, 6918.
(33) Baidak, A.; Naumov, S.; Brede, O. *J. Phys. Chem. A* **2008**, *112*, 10200.

JP9073569